

Femtosecond Probing of a 2c/3e Disulfide Bond Making in Liquid Phase

Y. Gauduel,* T. Launay, and A. Hallou

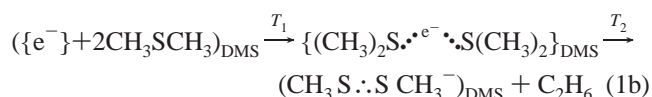
Laboratoire d'Optique Appliquée, INSERM U451, CNRS UMR 7639, Ecole Polytechnique-ENS Techniques Avancées, 91761 Palaiseau Cedex, France

Received: June 21, 2001; In Final Form: September 27, 2001

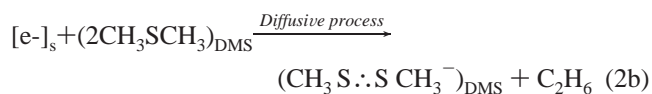
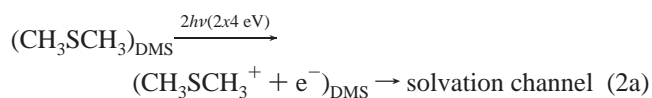
The subpicosecond ultraviolet observation of a sulfur–sulfur bond making ($2\sigma/1\sigma^*$ bond) is carried out in pure liquid dimethyl sulfide at 294 K. The early stages of a disulfide bonded radical formation ($\text{CH}_3\text{S}\cdot\text{:SCH}_3^-$) are characterized by a *nonlinear* λ_{max} red shift of the absorption spectrum. In the temporal range 0–1600 fs, the red shift of 0.31 ± 0.1 eV is analyzed in the framework of a change of the $2\sigma/1\sigma^*$ transition due to a lowering of the 2c,3e S–S bond strength and/or a destabilization of the σ lone pair during the demethylation process.

1. Introduction

The photochemistry of sulfur radical ions in liquids and solutions receives increasingly attention because they contribute to important oxidation–reduction processes in atmospheric sulfur cycle, solution chemistry and biochemistry.^{1–14} For instance, sulfur-centered intermediates involved in electron-transfer reactions act as a reducing agent, source of oxidant thiyl radicals, and may participate to S–S bond making/bond breaking in macromolecules.¹⁴ With organic sulfur compounds, the detection of short-lived electronic states provides some important basis for the microscopic investigation of elementary redox reactions.^{15,16} The one-electron reduction of sulfur compounds yields the formation of an odd-electron bond inside nascent sulfur-centered radical anions ($\text{RS}\cdot\text{:SR}^-$).^{17–21} Neat liquid dimethyl sulfide (DMS, CH_3SCH_3), the simplest of the thioethers, represents a paradigm for the short-time investigation of disulfide radicals anions characterized by the presence of a two-center three-electron bond (2c/3e bond). From femtosecond UV photoionization experiments of pure liquid DMS,²² it has been observed that, immediately after an electron photodetachment from a lone pair of sulfur atoms, a short-lived odd-electron bonded intermediate participates, via an efficient *electron attachment process*, to the subpicosecond formation of a disulfide radical anion $\text{CH}_3\text{S}\cdot\text{:SCH}_3^-$ (eq 1a,b). This radical is fully populated in less than 2 ps after the energy deposition in the liquid phase.



A second electron photodetachment channel leads to an electron solvation process and a subsequent diffusion-controlled radical reaction (eq 2a,b).



Complementary IR and UV femtosecond spectroscopic investigations raise that the second sulfur–sulfur radical anion formation channel takes place beyond 5 ps following the initial energy deposition in neat liquid dimethyl sulfide.²²

Regarding the subpicosecond formation of a disulfide radical anion $\text{CH}_3\text{S}\cdot\text{:SCH}_3^-$ in liquid environment (eq 1a,b), the exact configuration of a nonequilibrium precursor remains unknown and the general representation which is adopted $\{(\text{CH}_3)_2\text{S}\cdot\cdot\text{e}^- \cdot\text{S}(\text{CH}_3)_2\}_{\text{DMS}}$ includes the minimum of DMS molecules required for the formation of a sulfur–sulfur bond. This representation does not excluded that an early electron-monomer attachment followed by an ion–molecule reaction can take place or that an ultrafast electron trapping involves preexisting sulfur complexes. The time dependence of this UV intermediate argues for an ultrafast electron trapping in the DMS bath, an efficient electronic repartitioning between two sulfur atoms leading to a S $\cdot\cdot$ S $^-$ bond making and finally a molecular response via two C–S bond breakings (methyl abstractions). Previous experimental works emphasize that disulfide radical anions with a odd-electron bond are characterized by a UV absorption band centered around 3 eV (λ_{max}).^{4,5,20} This spectral signature is generally understood as an electronic transition between the uppermost doubly occupied orbital representing the σ energy level disturbed by a nonbonding sulfur electron and the singly occupied σ^* energy level.⁷

The femtosecond UV detections of a transient odd-electron bonded intermediate and a disulfide radical anion $\text{CH}_3\text{S}\cdot\text{:SCH}_3^-$ raises some fundamental questions about (i) the role of favorable angular orientation of the interacting p orbitals for an efficient electronic overlap of sulfur atoms and (ii) the reorganization energy inside the nascent disulfide bonded radical $\text{CH}_3\text{S}\cdot\text{:SCH}_3^-$. Does the unpaired electron and solvent caging change the degree of interaction between two sulfur moieties forming the $2\sigma/1\sigma^*$ bond?

* To whom correspondence should be addressed. Tel: +33 (0)1 69 31 97 26. Fax: +33 (0)1 69 31 99 96. E-mail: gauduel@ensta.fr.

The purpose of this experimental paper is to report some very detailed information on the early time events in the formation of a sulfur-centered radical anion $\text{CH}_3\text{S}\cdot\text{SCH}_3^-$ in pure liquid dimethyl sulfide. To establish whether an early spectral shift assists the subpicosecond $\text{S}\cdot\text{S}^-$ bond making, thorough investigations have been performed in the UV region. Femtosecond spectroscopic results provide useful information on the change of the $\sigma-\sigma^*$ energy level during the $2c/3e$ disulfide bond making and would open a new way to explore the stretching of the internuclear S–S distance of a parent σ bond on antibonding electron addition.

2. Experimental Section

Time-resolved UV spectroscopic experiments are performed with a pump–probe configuration. Femtosecond pulses centered at 620 nm are generated by a passively mode-locked CW dye ring laser. Amplified pulses of typically 80–90 fs duration and energy above 1 mJ are used to generate a second harmonic pump pulse with a KDP crystal ($6 \pm 0.5 \mu\text{J}$ at 310 nm) and a continuum (probe beam). Transient absorption signals are detected with Suprasil cells (1 mm path length). Dimethyl sulfide is obtained from Aldrich as 99,99% grade. Its purification over sodium and transfer distillation under vacuum into the experimental cell has been previously described.²² To avoid local heating and the accumulation of photoinduced products, the experiments were performed on Suprasil cell equipped with an expansion volume (~ 2 mL) and continuously moved so that each amplified laser pulse excites a new region of the liquid sample at 294 K.

An initial electron photodetachment is performed with femtosecond UV pulses (310 nm, 4 eV) by pumping in the low energy tail of DMS absorption band. The energy density of $6 \times 10^{10} \text{ W cm}^{-2}$ per pulse favors a two-photon absorption process. The short-time dynamics of photoinduced UV absorption signals are obtained with silicon photodiodes. For a given test wavelength, the transient signal is defined by 100 points and each point represents an average of 2×10^3 laser shots. The time dependence of an induced absorption signal is expressed by the physical response of the sample investigated by a computed photokinetic model and the correlation function between the excitation pulse (I_p) and the test beam (I_t) separated by a time delay τ . This correlation function represents the instrumental response that takes into account the pump–probe pulses temporal profiles and the overall broadening factor due to group velocity dispersion or refractive index effects in liquid samples.^{22,23} For a given test wavelength, the overall instrumental response is directly measured with neat nonpolar samples (*n*-heptane) for which an instantaneous UV signal rise time has been observed (Figure 1). In the same pump–probe configuration, short-time dependent UV spectra have been carried in the range 360–460 nm with an Optical Multichannel Analyzer (OMA 4) from Princeton Instruments. To avoid the dark current, the CCD detector is cooled with liquid nitrogen. The 1530-CUV sensor contains a matrix of 256×1024 pixels for which three tracks are defined. Two tracks are devoted to the measurement of test-reference beams and a third one to the reading noise. The amplitude of photoinduced UV signals being very small ($\Delta\text{OD} < 50 \times 10^{-3}$), a careful characterization of transient spectra is required. The acquisition of spectral data includes several procedures: photons countings with and without pump and direct measurements of group velocity dispersion in the liquid samples. The transient spectral data are defined with 35 positions of the stepping motor. To obtain a good coherence between spectroscopic measurements performed under photo-

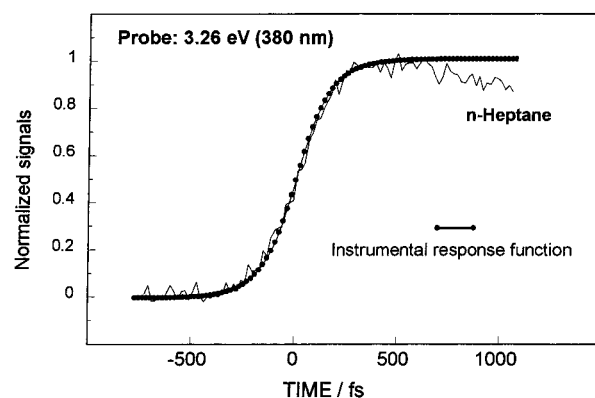


Figure 1. Overall instrumental response function defined in the ultraviolet (380 nm) by probing an “instantaneously” induced absorption signal following a biphotonic excitation of neat liquid *n*-heptane with femtosecond UV pulses (2×4 eV). The instantaneous signal rise time of prevailing spectral contributions due to excited state and molecular cation follows a deconvolution function that takes into account biexponential pump and probe beams of temporal pulse width of 140 fs.

diodes and CCD detector, dynamical and spectral experiments are performed in conditions for which the zero delay time is determined with an accuracy of 20–30 fs over a temporal window of 2 ps. Data acquisition and time-energy plot isosurfaces determined from CCD measurements between 360 and 460 nm are through custom software written in C²⁺. The large data sets are graphically treated with an Open Productivity Graphic System (OPGS).

3. Results and Discussion

a. Short-Time Characterization of Primary Events. The femtosecond UV experiments performed over a very short temporal window (2 ps full scale) require a careful cross checking of dynamical and spectral measurements obtained with different detectors. In a first step, the primary photophysical events triggered by femtosecond UV excitation of DMS molecules are probed with silicon photodiodes. The short-time spectroscopic measurements are reported in Figures 2 and 3. Immediately after the two-photon excitation of neat liquid DMS (2×4 eV) and the electron ejection from a sulfur $3p_x$ orbital occupied by a nonbonding lone pair, an early absorption signal is detected in the visible. At 640 nm (1.94 eV), the growing of the photoinduced absorption occurs within the response of the experimental system. This *instantaneous* signal rise time is assigned to an ultrafast formation of excited DMS cations ($\text{CH}_3\text{SCH}_3^+$)* for which a calculated absorption spectrum peaks in the visible.²²

The short-lived absorption signals detected in the UV (380, 400 nm) contain the signatures of primary radical anions. In agreement with a previous work,²² the signal probed at 380 nm (3.26 eV) contains the prevailing contribution of a short-lived component assigned to an odd-electron bonded intermediate $\{(\text{CH}_3)_2\text{S}\cdot\text{S}^{\cdot-}\cdot\text{S}(\text{CH}_3)_2\}_{\text{DMS}}$ (Figure 2). This transient state is characterized by a formation dynamics T_1 and a monoexponential relaxation time T_2 . The best computed fit of the experimental 380 nm curve gives $T_1 = 180 \pm 20$ fs and $T_2 = 270 \pm 20$ fs. In the framework of a two-state model, the time dependent $(\text{CH}_3)_2\text{S}\cdot\text{S}^{\cdot-}\cdot\text{S}(\text{CH}_3)_2$ population follows the expression:

$$[(\text{CH}_3)_2\text{S}\cdot\text{S}^{\cdot-}\cdot\text{S}(\text{CH}_3)_2](t) = A^\circ [T_2 / (T_2 - T_1)] [T_2 \exp(-t/T_2) - T_1 \exp(-t/T_1)] \quad (3)$$

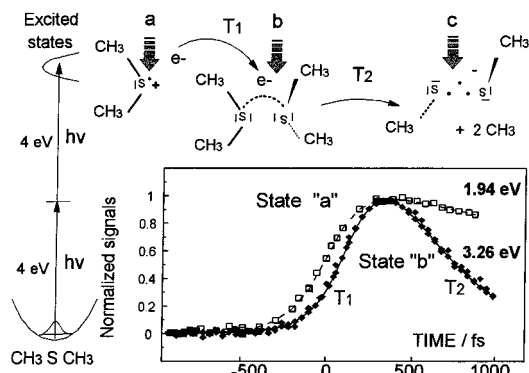


Figure 2. Early photochemical events involved in the ultrafast formation of a two-center, three-electron sulfur–sulfur bond ($2\sigma/1\sigma^*$ bond) following a femtosecond two-photon excitation (2×4 eV) of pure liquid dimethyl sulfide (CH_3SCH_3). Insert: Details of experimental curves probing an instantaneous rise time of a primary cation (state “a”) at 1.94 eV (640 nm) and the time dependence of a odd-electron bonded intermediate (state “b”) at 3.26 eV (380 nm). This short-lived state participates to the disulfide bonded radical formation (state “c”).

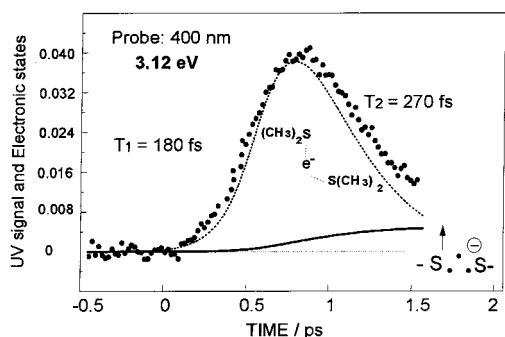


Figure 3. Short-time-dependence of photoinduced UV absorption signal following a femtosecond two-photon excitation of neat liquid DMS at 294K. At 400 nm, the contributions of a short-lived odd-electron bonded intermediate $\{(\text{CH}_3)_2\text{S}\cdot^{\ominus}\cdot\text{S}(\text{CH}_3)_2\}$ and a nascent anionic radical $(\text{CH}_3\text{S}\cdot\text{SCH}_3)^{\ominus}$ are reported (see text). The characteristic times T_1 and T_2 are defined by eqs 1–4.

Dynamical measurements performed at 380 nm emphasize that the transient odd-electron bonded intermediate would be populated for $\tau \sim 300$ fs (Figure 2). This nonequilibrium state is understood as a precursor of a UV sulfur-centered radical anion.

Additional investigations have been performed at longer wavelengths where disulfide radical anions are known to absorb.^{19,20,22} In this way, the transient signal probed at 400 nm (3.12 eV) is used to perform a cross checking of dynamical and spectral measurements (Figure 3). In the framework of a kinetic two state model, the photoinduced absorption signal is fitted to a linear combination of $(\text{CH}_3)_2\text{S}\cdot^{\ominus}\cdot\text{S}(\text{CH}_3)_2$ and $\text{CH}_3\text{S}\cdot\text{SCH}_3^{\ominus}$ contributions (eq 4).

$$\Delta A_{(t)}^{\omega} = \alpha[(\text{CH}_3)_2\text{S}\cdot^{\ominus}\cdot\text{S}(\text{CH}_3)_2]_{(t)} + \beta[\text{CH}_3\text{S}\cdot\text{SCH}_3^{\ominus}]_{(t)}, \quad \text{with } \alpha + \beta = 1 \quad (4)$$

In this equation, the dynamics of the $\text{CH}_3\text{S}\cdot\text{SCH}_3^{\ominus}$ population is expressed as follows:

$$[\text{CH}_3\text{S}\cdot\text{SCH}_3^{\ominus}](\tau) = A^{\circ}\{1 - 1/(T_1 - T_2)[T_2 \exp(-\tau/T_2) - T_1 \exp(-\tau/T_1)]\} \quad (5)$$

From the characteristic times previously defined at 380 nm ($T_1 = 180 \pm 20$ fs; $T_2 = 270 \pm 20$ fs), the expression 5 emphasizes that the neofomed $\text{CH}_3\text{S}\cdot\text{SCH}_3^{\ominus}$ radical level

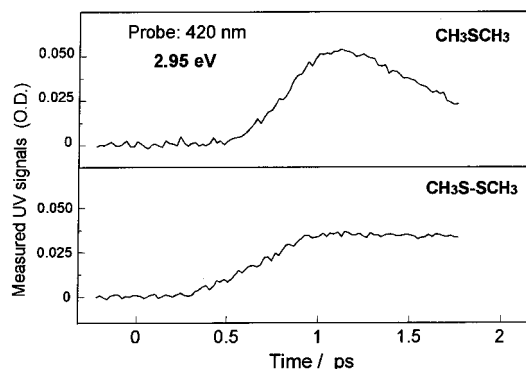


Figure 4. Short-time dependence of photoinduced absorption signals probed at 2.95 eV (420 nm) following the femtosecond UV excitation of neat liquid dimethyl sulfide (CH_3SCH_3) or dimethyl disulfide ($\text{CH}_3\text{S}-\text{SCH}_3$) at 294K.

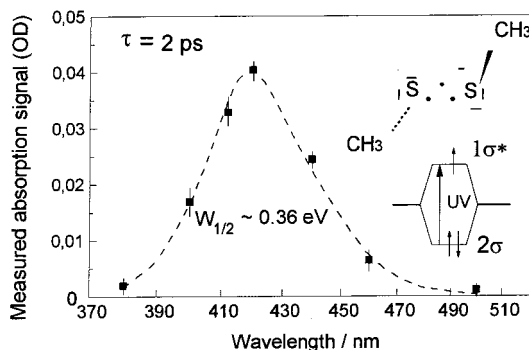


Figure 5. Transient UV absorption spectrum of a nascent three-electron-bonded radical anion ($\text{CH}_3\text{S}\cdot\text{SCH}_3^{\ominus}$) in pure liquid DMS at 294K. The points are determined from the experimental kinetics obtained with photodiodes and for a delay time of 2 ps. The dotted line is drawn as guide for the eyes. A simplified MO energy level scheme of the $2\sigma/1\sigma^*$ bonded radical is reported on the figure.

would maximize in less than 2 ps after the initial energy deposition (Figure 3). Indeed, the UV signature of the nascent disulfide radical anion represents $\sim 11\%$ of the signal contribution at 400 nm. It is interesting to point out that nascent disulfide radical anions ($\text{RS}\cdot\text{SR}^{\ominus}$) can be directly observed when the photoinduced electron transfer takes place in the presence of preexisting S–S bond.²¹ In the present work, this is the case with liquid dimethyl disulfide (DMDS, $\text{CH}_3\text{S}-\text{SCH}_3$) for which a photoinduced absorption signal probed at 420 nm (Figure 4) exhibits a ultrafast rise time assigned to disulfide radical anion ($\text{CH}_3\text{S}\cdot\text{SCH}_3^{\ominus}$).

In liquid DMS, a large fraction of the photoinduced UV signal includes the signature of the direct precursor of a disulfide radical anion. Consequently, the short-time formation of a $\text{CH}_3\text{S}\cdot\text{SCH}_3^{\ominus}$ radical is established by recording of magnitude of signal changes probed in the range 380–500 nm (3.26–2.48 eV). The photoinduced absorption spectrum reconstructed for a delay time of 2 ps is reported in Figure 5. The experimental UV absorption band peaks around 420 nm ($E_{\text{max}} \sim 2.97 \pm 0.02$ eV) and exhibits a half width ($W_{1/2}$) of ~ 0.36 eV. This early absorption spectrum is in good agreement with the UV spectrum of the long-lived sulfur–sulfur radical anion ($\text{CH}_3\text{S}\cdot\text{SCH}_3^{\ominus}$) observed in nanosecond experiments^{19,20} or predicted by calculated estimates in the picosecond regime.²² This UV absorption band is generally understood as a transition between the uppermost doubly occupied lone pair representing the σ energy level disturbed by a nonbonding sulfur electron and the singly occupied sulfur–sulfur σ^* orbital ($2\sigma/1\sigma^*$).^{7,14,17} To define whether some inhomogeneous spectral behaviors (shift

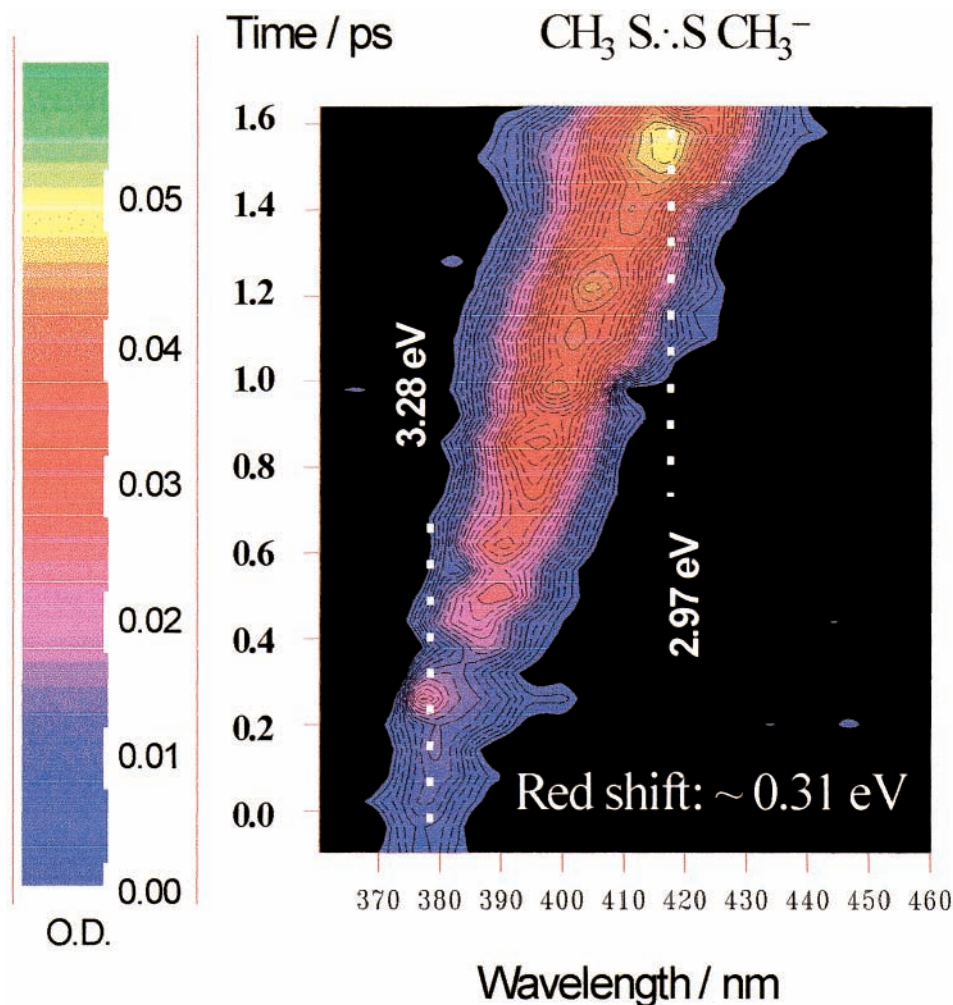


Figure 6. Two-dimensional measurements of a photoinduced absorption spectrum following the femtosecond two-photon excitation (2×4 eV) of pure liquid dimethyl sulfide. The spectral isosurfaces have been determined with a CCD matrix containing 1024 pixels for 100 nm of spectral range (0.1 nm/pixel) and 35 temporal steps of 60 fs. Considering that 5×10^2 laser shots have been used for each delay time, the final 2D mapping is obtained after the computed treatment of about 15×10^6 values. A short-time λ_{max} red shift is clearly observed during the rise time of the nascent anionic radical $\text{CH}_3\text{S}:\cdot\text{SCH}_3^-$.

or broadening) take place during the sulfur–sulfur bond making, a detailed investigation of this crucial point has been performed by probing the short-time UV spectra with an optical multi-channel analyzer equipped with a cooled CCD detector.

b. Short-time Frequency Dependence of a S:S Bond Making. The time-energy plot isosurfaces determined from CCD measurements between 360 and 460 nm (3.44–2.69 eV) are reported in Figure 6. Following the femtosecond energy deposition in neat liquid DMS, an early photoinduced absorption band centered around 378 nm ($\lambda_{\text{max}} \sim 3.28$ eV) appears in less than 300 fs. Subsequently, the spectral behavior follows the build up of a broader band. After a delay time of 1.6 ps, this band becomes centered at 417 nm ($\lambda_{\text{max}} \sim 2.97$ eV).

A comparison has been performed between these time-energy plot isosurfaces and time-resolved UV absorption signals analyzed with a kinetic two-state model (Figure 2,3). The transient band that early peaks around 378 nm (Figure 6) is assigned to the signature of a short-lived electronic state we name odd electron bonded intermediate $(\text{CH}_3)_2\text{S}:\cdot^{\ominus}\cdot\text{S}(\text{CH}_3)_2$. The photokinetic two-state model predicts that its level is maximum in the subpicosecond domain, typically around 350 fs at 380 nm (Figure 2). A good agreement is observed between this computed estimate, which remains model dependent, and the subpicosecond spectral profile reported in Figure 6. We conclude that *the short-lived absorption band that peaks initially around*

378 nm (3.28 eV) contains the early UV sulfur radical anion $(\text{CH}_3)_2\text{S}:\cdot^{\ominus}\cdot\text{S}(\text{CH}_3)_2$, i.e., a fleeting precursor of a disulfide radical anion. Physically speaking, this anionic radical precursor is understood as a very unstable intermediate for which an excess electron becomes transiently localized by preexisting sulfur complexes. When the microscopic structure of the reaction area is modified by the presence of additional solute, the odd-electron bonded intermediate $\{(\text{CH}_3)_2\text{S}:\cdot^{\ominus}\cdot\text{S}(\text{CH}_3)_2\}_{\text{DMS}}$ channel is significantly attenuated.²⁴ In pure liquid DMS, an early electron self-trapping would permit a partial overlap of sulfur $3p_x$ orbital occupied by nonbonding lone pair of electron. The build-up dynamics of this nonequilibrium electronic state substantiates an efficient interaction of the excess electron with a nascent σ sulfur–sulfur bond.

The salient feature of our spectral detection performed in the range 360–460 nm concerns the direct observation of a continuous *red shift* during the formation of a nascent σ sulfur–sulfur radical anion $\text{CH}_3\text{S}:\cdot\text{SCH}_3^-$ (Figure 6). For a delay time of 1.6 ps, the position of λ_{max} at 417 nm (2.97 eV) agrees with the UV absorption spectrum determined by photodiodes (Figure 5). Although the kinetic two-state model does not take into account the existence of a short-time spectral displacement, it predicts that the $\text{CH}_3\text{S}:\cdot\text{SCH}_3^-$ radical is mainly populated within the first 2 ps after the initial energy deposition (Figure 3). In the present study, the *subpicosecond continuous*

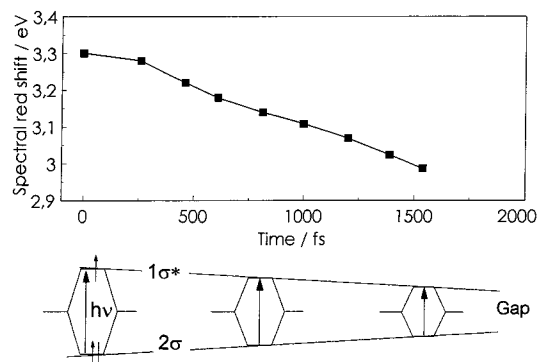
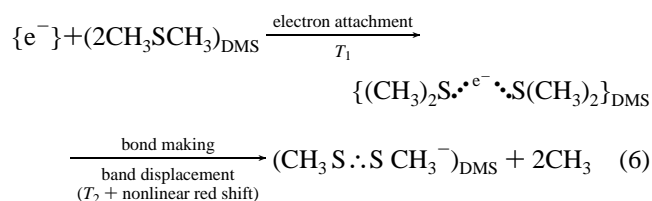


Figure 7. Real-time probing of a nonlinear λ_{\max} red shift that parallels the build-up of a nascent disulfide radical anion $\text{CH}_3\text{S}\cdot\cdot\text{SCH}_3^-$ in neat liquid DMS. The time dependent *red shift* in optical absorption is assigned to a smaller difference between the 2σ and $1\sigma^*$ energy level of the two-center-three-electron ($2\sigma/1\sigma^*$) bond.

red shift substantiates that the ultrafast $\text{S}\cdot\cdot\text{S}^-$ bond formation does not entirely obey to a simple two-state model and involves some additional spectral behaviors (shift and broadening) of $\{(\text{CH}_3)_2\text{S}\cdot\cdot\text{S}(\text{CH}_3)_2\}_{\text{DMS}}$ and $\text{CH}_3\text{S}\cdot\cdot\text{SCH}_3^-$ bands. From the subpicosecond-energy plot isosurfaces reported in Figure 6, the following sequence is proposed (eq 6).



The short time spectral red shift that parallels the subpicosecond formation and stabilization of a sulfur-centered radical anion $\text{CH}_3\text{S}\cdot\cdot\text{SCH}_3^-$ in liquid DMS does not question the validity of spectral assignments established with a two state model.²² In agreement with our previous conclusions, the femtosecond electron attachment channel involved in this ultrafast $\text{CH}_3\text{S}\cdot\cdot\text{SCH}_3^-$ formation is governed by a odd-electron-bonded intermediate that absorbs in the spectral range 370–460 nm. The relaxation of this transient electronic state ($\{(\text{CH}_3)_2\text{S}\cdot\cdot\text{S}(\text{CH}_3)_2\}_{\text{DMS}}$) parallels the subpicosecond formation of a nascent disulfide radical anion. However, due to technical UV limitations of the previous study, we could not completely precluded the existence of spectral inhomogeneities during the $\text{CH}_3\text{S}\cdot\cdot\text{SCH}_3^-$ formation. The present work substantiates clearly that the charge repartitioning between organic sulfur molecules during the SS bond making is simultaneously assisted by a subpicosecond UV band displacement. Consequently, in the temporal range 0–700 fs, the spectral red shift explains the slight discrepancy we observed between the UV signal rise time probed at 400 nm and the best computed data obtained with a kinetic two-state model (Figure 3).

Let us focus our attention on a key point raised by the real-time probing of a continuous red shift that parallels the $\text{CH}_3\text{S}\cdot\cdot\text{SCH}_3^-$ formation. From two-dimensional measurements reported in Figure 6, the real time observation of λ_{\max} permits the discrimination of a *nonlinear* spectral red shift (Figure 7). A large fraction of the λ_{\max} displacement (~ 75 –80%) takes place in the temporal range 500–1500 fs. The femtosecond probing of this λ_{\max} red shift can be discussed by considering available literature data devoted to the sulfur–sulfur bond electronic structure.^{20,25–27} Experimental studies and ab initio calculations on the UV absorption signature of two-center-three-

electron bonds as in $(\text{RS}\cdot\cdot\text{SR}^-)$ emphasize that the λ_{\max} position is generally understood as a transition between the uppermost occupied lone pair representing the σ energy level disturbed by a nonbonding sulfur electron and a singly occupied sulfur–sulfur σ^* orbital. That means that the level of interaction between two atomic cores forming a two-center-three-electron bond can be related to the amplitude of the σ – σ^* orbitals splitting. In the presence of an unpaired electron, the energy of a $2\sigma/1\sigma^*$ three electron bond ($\text{S}\cdot\cdot\text{S}$) is lower than that of a σ bond.^{25,26} Consequently, an energy difference $a_g \{ \sigma - n' \} / b_u$ (σ^*) of 2.5–3 eV would correspond to a UV transition.^{20,26} In agreement with these predictions, the UV signature of a nascent disulfide radical ion $\text{CH}_3\text{S}\cdot\cdot\text{SCH}_3^-$ in liquid DMS peaks around 417–420 nm (Figure 5,6).

The subpicosecond stabilization of a disulfide radical anion from a transient odd electron bonded intermediate $(\text{CH}_3)_2\text{S}\cdot\cdot\text{S}(\text{CH}_3)_2$ raises (i) the role of favorable angular orientation of the interacting p orbitals for an efficient orbital overlap and (ii) *the limited effect* of solvent relaxation around the newly created disulfide radical anion. The present study permits to clearly establish that even if a slight blue-shift originating from a sudden change of forces coupling the neofomed disulfide radical anion $\text{CH}_3\text{S}\cdot\cdot\text{SCH}_3^-$ to surrounding DMS molecules takes places at the subpicosecond time scale (solvation process), this effect does not prevail and is largely dominated by a red shift in the temporal range 0.3–1.6 ps. Consequently, we tentatively conclude that the time dependent λ_{\max} displacement toward the long wavelengths cannot be analyzed in the framework of a correlation function that would be governed by dielectric relaxation of solvent molecules in the vicinity of the nascent anionic radical $\text{CH}_3\text{S}\cdot\cdot\text{SCH}_3^-$.

We reasonably interpret this subpicosecond red shift as an indicator of the electronic structure reorganization of the transient $\{(\text{CH}_3)_2\text{S}\cdot\cdot\text{S}(\text{CH}_3)_2\}_{\text{DMS}}$ complex (Figure 2). One aspect of the short-time reorganization energy of this complex concerns a demethylation process.⁷ The methyl loss can be seen as a driving force of the S–S bond making. During the breaking of a S–CH₃ bond whose the energy is around 3.35 eV,²⁸ we cannot exclude a time dependent effect of the methyl loss on the energy of the sulfur 3p_x occupied by a non bonding lone pair of electrons. In this way, the subpicosecond λ_{\max} red shift would trend toward (i) a destabilization of the σ lone pair orbital triggered by a change of the bonding electrons engaged in 3s–3p hybridized orbital (methyl abstraction) and (ii) a subsequent decrease of the energy gap between the non bonding lone pair of electrons which is perpendicular to the S–S axis and the σ^* orbital which is parallel to the S–S axis.

A second explanation of the subpicosecond nonlinear λ_{\max} red shift can be contemplated in the framework of a weakening of the 2c–3e S–S bond strength. For different sulfur-centered anionic radicals, Asmus et al. have previously established a linear correlation between the optical absorption transition and Taft's induction σ^* parameter.^{20,29} These authors emphasize that the position of the maximum UV absorption band (λ_{\max}) could be an indicator of the $\text{S}\cdot\cdot\text{S}^-$ bond strength. As far as our experimental data concerns the real time probing of a 2c–3e disulfide bond making, we cannot exclude a correlation between the short-time λ_{\max} position of the absorption band and a decrease in the splitting magnitude between an orbital characterized by a strong σ lone pair and a σ^* orbital having a “p” lone pair character. During the temporal range 500–1500 fs for which a large fraction of disulfide radical anion $\text{CH}_3\text{S}\cdot\cdot\text{SCH}_3^-$ is populated (Figure 3), a λ_{\max} displacement of 0.2 eV is observed (Figure 7). This red shift in optical absorption (~ 20

meV/100 fs) would trend a *weakening of the nascent 2c–3e S⋮S bond* and the corresponding *smaller difference between the σ and σ^* energy levels after the odd-electron addition*. In other words, the subpicosecond λ_{\max} red shift would reflect the influence of a substituents repartitioning that occurs during the demethylation process on the strength of the three-electron bond. In this way, the methyl abstraction would favor a lowering of the degree of interaction between two moieties involved in the nascent S–S bond. The conversion of short-time spectral data into information on molecular geometries represents an interesting and worthwhile problem for future investigations on the nuclear coordinates of transient radical intermediates in molecular liquids.

4. Concluding Remarks

Despite the interest in 2c–3e S⋮S bonded radicals for chemistry and biology, very few experiments have directly probed the nature of these bonds. Femtosecond spectroscopy of photoinduced elementary anionic radical reactions in neat dimethyl sulfide enables us to give some detailed information on the short-time position of a UV absorption band that parallels the formation of a sulfur–sulfur radical anion $\text{CH}_3\text{S}\cdot\cdot\text{SCH}_3^-$. For the first time, the direct probing of the 2c/3e sulfur–sulfur bond making ($2\sigma/1\sigma^*$ bond) from a short-lived odd-electron bonded intermediate raises the existence of a *femtosecond nonlinear λ_{\max} red shift*. This spectral displacement is interpreted in the framework of an early change of the $2\sigma/1\sigma^*$ transition due to a lowering of the 2c,3e S–S bond strength and/or a destabilization of the σ lone pair during the methyl abstraction.

To the best of our knowledge, any semiquantum MD simulations devoted to an electron localization in liquid DMS or to a short-lived precursor of $\text{CH}_3\text{S}\cdot\cdot\text{SCH}_3^-$ radical are available. The present femtosecond spectroscopic data provide some experimental basis on which MD simulations and statistical mechanics would be used (i) to investigate the role of the density fluctuations of a liquid thioether on the early electron–sulfur molecule couplings (time-dependent affinity of DMS molecules for an excess electron) and (ii) explore the quantum mechanical character of $2\sigma/1\sigma^*$ S⋮S bond.^{25–30} Regarding the charge and energy repartitioning within a nascent bond of chemical and biological interest, we should wonder whether (i) the loss of two substituents abstraction inside a short-lived odd-electron bonded intermediate $\{(\text{CH}_3)_2\text{S}\cdot\cdot\cdot\text{S}(\text{CH}_3)_2\}_{\text{DMS}}$ increases the internal rotation of the moieties and allow a more favorable overlap of hybridized p_x orbital for S–S bonding, (ii) the σ^* energy level is influenced by other orbitals during the methyl abstraction and (iii) the observed subpicosecond λ_{\max} red shift of 0.31 eV trends a stretching of the internuclear SS distance of a parent σ bond on antibonding electron addition.

Acknowledgment. This work was supported by INSERM, the Chemical Department of CNRS–GdR 1017, France, and the Commission of the European Communities.

References and Notes

- (1) Kosower, N. S.; Kosower, E. M. In *Free Radicals in Biology*; Pryor W. A., Ed.; Academic Press: London, 1976; Vol. 2, pp 55–84.
- (2) Armstrong, D. A.; Chipman, D. M. In *S-Centered Radicals*; Alfassi, Z. B., Ed.; Wiley: Chichester, 1999; pp 1–26. Armstrong, D. A. In *S-Centered Radicals*; Alfassi, Z. B., Ed.; Wiley: Chichester, 1999; pp 27–61.
- (3) Bisby, R. H.; Cundall, R. B.; Redpath, J. L.; Adams, G. E. *J. Chem. Soc., Faraday Trans. 1* **1976**, 72, 51.
- (4) Asmus, K. D.; Bahnemann, D.; Fischer, C. H.; Veltwisch, D. *J. Am. Chem. Soc.* **1979**, 101, 5322.
- (5) Göbl, M.; Bonifacic, M.; Asmus, K. D. *J. Am. Chem. Soc.* **1984**, 106, 5984.
- (6) Chaudri, A. A.; Göbl, M.; Freyholdt, T.; Asmus, K. D. *J. Am. Chem. Soc.* **1984**, 106, 5988.
- (7) Chatgililoglu, C.; Asmus, K. D., Eds. *Sulfur-Centered Reactive Intermediates in Chemistry and Biology*; Plenum Press: New York, 1990.
- (8) Charlson, R. J.; Lovelack, J. E.; Andreae, M. O.; Warren, S. G. *Nature* **1987**, 326, 655.
- (9) Yin, F.; Grosjean, D.; Seinfeld, J. H. *J. Atmos. Chem.* **1990**, 11, 309.
- (10) Tyndall, G. S.; Ravishankara, A. R. *Int. J. Chem. Kinet.* **1991**, 23, 483.
- (11) Turnipseed, A. A.; Barone, S. B.; Ravishankara, A. R. *J. Phys. Chem.* **1986**, 96, 7502.
- (12) Syage, J. A.; Pollard, J. E.; Cohen, R. B. *J. Phys. Chem.* **1991**, 95, 8560.
- (13) Barone, S. B.; Turnipseed, A. A.; Ravishankara, A. R. *J. Phys. Chem.* **1996**, 100, 14703.
- (14) Alfassi, Z. B., Ed. *S-Centered Radicals*; Wiley: Chichester, 1999; p 27.
- (15) Armstrong, D. A. In *Sulfur-Centered Reactive Intermediates in Chemistry and Biology*; Chatgililoglu, C., Asmus, K. D., Eds.; Plenum Press: New York, 1990; pp 341–351.
- (16) Zhong, D.; Zewail, A. H. *Proc. Natl. Acad. Sci. U. S. A.* **1999**, 96, 2602.
- (17) Baird, N. C. *J. Chem. Educ.* **1977**, 54, 291.
- (18) Marignier, J. L.; Belloni, J. *J. Phys. Chem.* **1981**, 85, 3100.
- (19) Belloni, J.; Marignier, J. L.; Katsumura, Y.; Tabata, Y. *J. Phys. Chem.* **1986**, 90, 4014.
- (20) Asmus, K. D. In *Sulfur-Centered Reactive Intermediates in Chemistry and Biology*; Chatgililoglu, C., Asmus, K. D., Eds.; Plenum Press: New York, 1990; pp 155–172.
- (21) Gauduel, Y.; Gelabert, H.; Guilloud, F. *J. Am. Chem. Soc.* **2000**, 122, 5082.
- (22) Gauduel, Y.; Marignier, J. L.; Belloni, J.; Gelabert, H. *J. Phys. Chem. A* **1997**, 101, 8979.
- (23) Gauduel, Y. *J. Mol. Liq.* **1995**, 63, 1.
- (24) Gauduel, Y.; Hallou, A. In preparation.
- (25) Clark, L. B.; Simpson, W. T. *J. Chem. Phys.* **1965**, 43, 3666.
- (26) Clark, T. *J. Am. Chem. Soc.* **1988**, 110, 1672.
- (27) Deng, Y.; Illies, A. J.; Jame, M. A.; McKee, M. L.; Peschke, M. *J. Am. Chem. Soc.* **1995**, 117, 420.
- (28) McMillen, D. F.; Golden, D. M. *Annu. Rev. Phys. Chem.* **1982**, 33, 493.
- (29) Asmus, K. D.; Bonifacic, M. In *S-Centered Radicals*, Alfassi, Z. B., Ed.; Wiley: Chichester, 1999; p 141.
- (30) Senent, M. L.; Moule, D. S.; Smeyers, Y. G. *J. Phys. Chem.* **1995**, 99, 7970.